International Engineering Journal For Research & Development
Vol.5
Issue 7
E-ISSN NO:-2349-0721
Impact factor : 6.549

USE OF SPLINE FUNCTIONS IN CARDIOLOGY PROCESSES

Abdurasulova Dilnoza Botirali qizi
Republic of Uzbekistan, Ferghana region Ferghana branch of Tashkent information technologies university named after Mukhammad al Kharazme, 2 course masters degree faculty of computer engineering
abdurasulova-d@mail.ru

ABSTRACT

Due to their minimal invasiveness catheters are highly preferred incardiacmapping techniques used in the source localization of rhythm disturbances in the heart. In cardiac mapping, standard steerable catheters and multielectrode basket catheters are the two alternatives for the characterization of the underlying tissue on the inner (endocardium) and outer (epicardium) surfaces of the heart. As with any discrete sampling technique, an important question for catheter-based cardiac mapping is how to determine values at locations from which direct measurements are not available. Interpolation is the most common approach for providing values at unmeasured sites using the available measurements. In this study, the usage of spline interpolation technique in catheter-based cardiac mapping was introduced for the first time in the literature and compared with the existing approaches such as the nearest-neighbor, Laplacian, and Hardy's interpolation techniques.

For different sampling resolutions on the endocardium and epicardium, we reconstructed the activation-time values on unmeasured sites using measured values. To provide quantitative validation, we have applied thesemethods to high resolution simulated activation-time values from a realistic heart model using Aliev-Panfilov mathematical modeling approach. The results show that spline, Laplacian, and Hardy interpolation methods performed successfully and also better than nearest-neighbor method. Among all interpolation schemes exceptfor the nearest-neighbor method the average correlation coefficient (CC) values were greater than

Key Words: ***Surface interpolation, spline interpolation, catheter-based cardiac mapping, computer simulation.***

INTRODUCTION

The purpose of an electrophysiological (EP) study is that it offers more detailed information to the doctor about the electrical activity in the heart than various noninvasive tests such as ECG, holter, stress test, Turk J Elec Eng & Comp Sci, Vol.18, No.6, 2010 echocardiography, because electrodes are placed within the heart chambers and the coronary vessels, or on the outer surface of the heart (epicardium). This allows an electrophysiologist to determine the specific locationof the source of an arrhythmia and, oftentimes, correct it during the same procedure by applying energy to the arrhythmogenic tissue. This corrective treatment is permanent and considered a cure, and, in many cases, the patient may not need to take arrhythmia related medications. Refinements in mapping techniques have allowed the development of highly effective catheter-basedtechniques for ablation of most types of supraventricular tachycardia as well as different kinds of ventricular tachycardia (VT). These mapping techniques, including electroanatomic mapping and noncontact endocardial mapping, nowadays replaced intraoperative direct mapping, which is now rarely performed.However, most of these approaches require high first-establishment costs and expensive procedures due to the sophisticated hardware and specialized catheters.The most common clinical method to identify

regions that support VT for ablation utilizes roving catheters and the standard 12-lead ECG. Preliminary arrhythmia source localization is typically achieved through analysis of a 12-lead ECG during sinus rhythm. To refine the location, multipolar catheters arepositioned within the coronary sinus, tricuspid, or mitral annuli. Final localization and ablation is then achieved through mapping with a steerable endocardial catheter. Many of the complex forms of VT are especially difficult to recognize using a single steerable catheter. For the proper characterization of the arrhythmogenic areas it may be necessary to increase the procedure times by sampling the ventricles in a more detailed manner. Increasing the procedure times leads to the increase in the ionizing radiation exposure due to the fluoroscopy system used in the EP laboratories. It is also possible to apply endocardial or epicardial mapping through the use of multielectrode basket catheters and intravenous catheters. The most basic questions in acquiring cardiac potential data involve selecting the number and position of recording electrodes necessary to adequately capture a potential distribution and/or activation-time distribution. With a limited acquisition bandwidth, there is a constant trade-off between spatial sampling density and coverage.

Spline interpolation was developed previously in the context of geophysics [13], and was later extended to electroencephalography (EEG). A general form of splines introduced to EEG by Perrin et al. [14] for interpolating two-dimensional polar projections of EEG data, and then extended to three-dimensional scalpsurfaces by Law et al. [15] and Srinivasan et al. [16]. Several cardiac applications of spline interpolation include heart surface geometry reconstruction [17], image reconstruction [18], and inverse electrocardiography [19]. In this study, the usage of spline interpolation technique in catheter-based mapping of both epicardiumand endocardium was introduced for the first time in the literature and compared with the existing approaches such as the nearest-neighbor, Laplacian, and Hardy's interpolation techniques. For different sampling resolutions, we reconstructed the activation-time values on unsampled sites. To provide quantitative validation, wehave applied these methods to high resolution simulated activation-time values from a geometric heart model (Auckland heart) using Aliev-Panfilov mathematical modeling approach [20]. In selecting surrogate measurement sites on the endocardium we assumed that certain percentage of all sites obtained by roving catheter or 64 sites on the left or right ventricular surface obtained by multielectrode basket catheter were accessible. In addition, multielectrode venous catheter measurements or roving catheter in the pericardial space were assumedas accessible and the activation-time values on the remaining sites were interpolated. Finally, the interpolation results and the original activation-time maps on the endocardial and epicardial surfaces were compared usingthe statistical criteria such as correlation coefficient, root-mean-squared error, and relative error.

2. METHODS

2.1. Simulation database

We performed cardiac simulations using "Aliev-Panfilov model" [20–22] to create the simulation database.

AlievPanfilov model is a modified FitzHugh-Nagumo (FHN) model and composed of a pair of differential equations defining fast and slow processes:

$$\frac{\partial u}{\partial t} = \frac{\partial}{dx_i} \cdot d_{ij} \cdot \frac{\partial u}{\partial x_j} - ku(u-a)(u-1) - uv$$

$$\frac{\partial v}{\partial t} = \varepsilon(u,v)(-v - ku(u-a-1)) \quad (1)$$

Here, $\varepsilon(u, v) = \varepsilon 0 + \mu 1v/(u + \mu 2)$, and u and v are fast and slow variables, respectively. Conductivity tensor dij shows the fiber directions. We first discretized the equations above and solved them iteratively for all points on the simulation geometry, with $k = 8$, $a = 0.15$, $\varepsilon 0 = 0.002$, $\mu 1 = 0.2$, $\mu 2 = 0.3$, $\Delta x = 0.6$, and $\Delta t = 0.07$ [22,23].

The computer simulation geometry was composed of the ventricles of the Auckland canine heart model. For this geometry the coordinate and fiber orientation information have been obtained by Nielsen et al. [24]. Turk J Elec Eng & Comp Sci, Vol.18, No.6, 2010 In this work we used an interpolated version of the raw geometry data containing 532552 heart points. We created a subset of these points which included 2590 points on the epicardial and endocardial surfaces. These points were regularly distributed on the left (562 points) and right endocardial (488 points) surfaces, and on the epicardial surface (1590 points). The simulations were started from these sites (by activating each site and the neighboring 14 other points on the 532552 point geometry) one by one, and thus, for each simulation we obtained 532552 activation-time values on all heart points. For each point on the simulation geometry we computed the activation-time value as the time of $u$variable reaching the value 0.7. The activation-time values on the starting points were assumed to be zero millisecond. Each simulation result corresponded to a focal arrhythmic activity on the ventricles. We then extracted the activation-time values from 2590 points for each computer simulation and thereby constructed the simulation database, a 2590-by-2590 matrix, for the interpolation study.

2.2. Surrogate catheter measurements

In order to test performances of each interpolation method on the endocardial mapping we selected a subset of the sites on the left and right endocardial surfaces of the simulation geometry. These sites served as the sparse measurements obtained by roving catheter steered in the cardiac chambers. The selected sites were regularly distributed over the surfaces and comprised 5%, 10%, or 20% of all sites on the corresponding chamber. To simulate the clinical usage of multielectrode basket catheter (MBC), we selected 64 sites on the left and 64 sites on the right endocardial surfaces. For epicardial mapping, we selected 5%, 10%, or 20% of the 1540 epicardial sites on the simulation geometry. These sites were also regularly distributed. To simulate the clinical usage of multielectrode venous catheters (MVC) we selected 91 sites on the epicardium of the simulation geometry, which corresponded to the great coronary veins such as coronary sinus, middle cardiac vein, left ventricular posterior vein, and great cardiac vein.

2.3. Interpolation

In three-dimensional space, if the values measured at such N points as (xi, yi, zi), $i = 1, 2, \ldots, N$, are known as qi, the general interpolation problem can be defined as determining T(x, y, z) function such that [25],

$T(xi, yi, zi) = qi$, for $i = 1, 2, \ldots, N$. (2)

Determining T(x, y, z) within the finite dimensional linear interpolation space, which has the general form of

$$T(xi, yi, zi) = \Sigma ci\varphi i(x, y, z), \text{ for } i = 1, 2, \ldots, M, \quad (3)$$

where $\varphi i(i = 1, 2, \ldots, M)$ is a set of basis functions and the coefficients, ci, are determined by the interpolation conditions. With basis functions and coefficients, $T(x, y, z)$ gives a complete description of the underlying spatial

distribution. Therefore, this function can be used to estimate the value at any unsampled site at (xp, yp, zp) using equation,

$$qp = T(xp, yp, zp) = \Sigma ci\varphi i(xp, yp, zp), \text{ for } i = 1, 2, \ldots, M. \quad (4)$$

2.3.1. Nearest-neighbor interpolation method

The nearest-neighbor (NN) interpolation is a simple method. The activation-time value interpolated at a given point p on the cardiac surface is the weighted sum of the activation-time values attributed to each of the measurement sites. The weight attributed to each site is a function of the Euclidean distance between this site and the point *p*. We experimented with different number of neighbors and found that 6 is the best value for this problem. The estimated activation-time value for point *p* for the 6 nearest measurement sites is given by the relation $qp = \Sigma qid\text{-}\ i\ 1/\Sigma d\text{-}\ i\ 1$, for $i = 1, 2, \ldots, 6$. (5) where $di = (xp - xi)2 + (yp - yi)2 + (zp - zi)2$ and qi is the activation value and xi, yi , and zi are thecoordinates at the *ith* measurement site.

2.3.2. Laplacian interpolation method

In the Laplacian interpolation method, first, a local approximation of the surface Laplacian is defined over all the points in the geometry, secondly, the values at unsampled points in the geometry are adjusted so as to globally minimize the Laplacian [9]. This approach achieves maximum smoothness of the entire distribution, thereby avoiding any new extrema or regions of sharp spatial gradient. The local approximation requires a mesh of the scattered data points, from which the first order neighbors for each point are determined as

$$\nabla^2 q_0 \approx \frac{4}{\bar{d}} \left(\frac{1}{n} \sum_{i=1}^{n} \frac{q_i}{d_i} - \left(\frac{\bar{1}}{d} \right) q_0 \right), \quad (6)$$

where di is the distance between the node at which the potentials are interpolated and i*th* neighbor with value qi, $-d$ is the mean distance to all n neighbors, and 1 d is the mean inverse distance to all n neighbors. Average n was 6 for this method.

2.4. Hardy's interpolation method

Hardy's interpolation method is a global, continuously differentiable interpolation method for solving scattered data interpolation problems. It is capable of producing monotonic, extremely accurate interpolating functions, integrals, and derivatives. This method was originally developed to produce topographical maps from sparse, scattered data for surveying and geographic mapping. Since its development this method has evolved into a general purpose interpolation scheme for multivariate data in diverse fields of science and engineering. Hardy'smethod uses multiquadric radial basis functions which depend on the Euclidean distance from the point p at which the value is interpolated to the sampled points, di, with a shift of R. This function has the form

$$T(x_p, y_p, z_p) = \sum_{i=1}^{N} c_i \sqrt{d_i^2 + R^2}, \quad (7)$$

We used the global implementation of the Hardy's interpolation method, i.e., we used all the values at the measurement sites (N points) to determine T(p). Using the distances between the measured values *ci* coefficients were computed [8]. We experimented with different R values and found that $R = 0$ was the best value for this problem.

2.4.1. Spline interpolation

The three-dimensional (3D) spline interpolation function is defined as the following:

$$q(r) = Q_{m-1}(r) + \sum_{i=1}^{N} q_i K_{m-1}\left(|r - r_i|^2\right), \tag{8}$$

where K_{m-1} is a basis function [26, 27],

$$K_{m-1}\left(|r - r_i|^2\right) = \left(|r - r_i|^2\right)^{m-1} \log\left(|r - r_i|^2\right), \tag{9}$$

and Q_{m-1} is a 3D polynomial of order m-1,

$$Q_{m-1}(r) = \sum_{d=0}^{m-1} \sum_{k=0}^{d} \sum_{g=0}^{k} q_{dkg} (x)^{d-k} (y)^{k-g} (z)^{g}. \tag{10}$$

The *Qm*-1 is known as an osculating function, which constraints the smoothness of the interpolation of the resulting surface distribution; *N* is the total number of catheter measurements available; and *qi* is the activationvalue measured at the *ith* catheter electrode. We experimented with different m values and the best *m* was found to be 3 in this problem.

2.5. Statistical comparison

In order to compare the original activation-time maps with the results of the interpolation method we used three metrics: correlation coefficient (CC), root-mean-squared error (RMSE), and relative error (RE) [28]:

$$CC = \frac{\sum_{i=1}^{U} \left(q_i^m - \overline{q^m}\right)\left(q_i^e - \overline{q^e}\right)}{\sqrt{\sum_{i=1}^{U} \left(q_i^m - \overline{q^m}\right)^2} \sqrt{\sum_{i=1}^{U} \left(q_i^e - \overline{q^e}\right)^2}} \tag{11}$$

$$RMSE = \sqrt{\frac{\sum_{i=1}^{U} \left(q_i^e - q_i^m\right)^2}{U}} \tag{12}$$

$$RE = \sqrt{\frac{\sum_{i=1}^{U} \left(q_i^e - q_i^m\right)^2}{\sum_{i=1}^{U} \left(q_i^m\right)^2}} \tag{13}$$

where *qie* and *qim* are the interpolated and simulated activation-time values at the *ith* unsampled site, and *qm* and *qe* is the average of all interpolated activation-time values. *U* is the number of unsampled sites on which the interpolated values were computed.

RESULTS

Table 1 indicates that the interpolation performance improved as the number of surrogate catheter measurements increased. Among all interpolation schemes, except for the nearest-neighbor method, the average correlation coefficient (CC) values were greater than 0.985, the average root-mean squared error (RMSE) was less than 2.9

ms, and the average relative error (RE) was less than 0.07 (or 7%). The Laplacian, Hardy's, and spline interpolation approaches performed similarly with each other and outperformed nearest-neighbor method for all resolutions and catheter types. These three methods resulted in similarly accurate activation-time maps for 5% spatial resolution and MBC on the left and right endocardial surfaces. The performances when 5% spatial resolution and MBC were used were slightly worse than 10 and 20% resolutions. The interpolation methods applied on the left and right endocardial surfaces did not yield significantly different results. A slightly better performance has been noted on the right endocardium, maybe because of the less complex model geometry when compared to left endocardium. An observation which is consistent with this was that the interpolation approaches tested on the epicardial surface resulted in highly accurate activation maps for all surrogate roving catheter measurements. When the highly sparse MIVC was used to obtain the epicardial activation maps the worsening in the performance was obvious, however, again in the range of 0.950 as the correlation coefficient values. The nearest-neighbor method's performance did not reach to an acceptable level for the MIVC usage on the epicardial surface.

Figure 1, 2, and 3 show the examples of original and interpolated activation maps for the epicardially, left and right endocardially stimulated maps, respectively. Dark blue and dark red show the earliest and latest

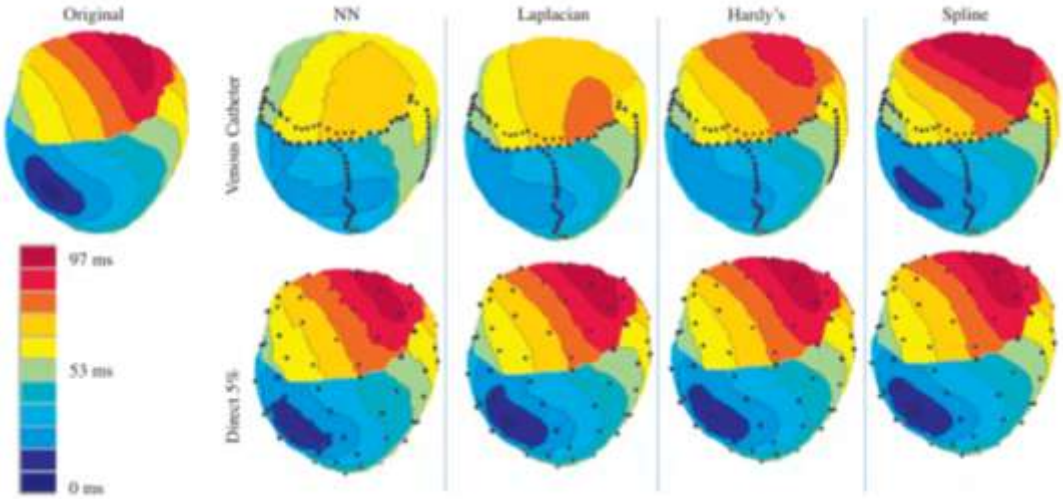

Figure 1. The original activation-time map and the interpolation results of nearest neighbor, Laplacian, Hardy's, and spline approaches on the epicardium (Epi) when the simulation was initialized from a site on the left anterior epicardium.

The surrogate measurements were taken from the 91 venous catheter (MIVC) sites and the sites that were regularly distributed over the epicardium and constituted only the 5% of all sites (corresponding to the usage of steerable single catheter).

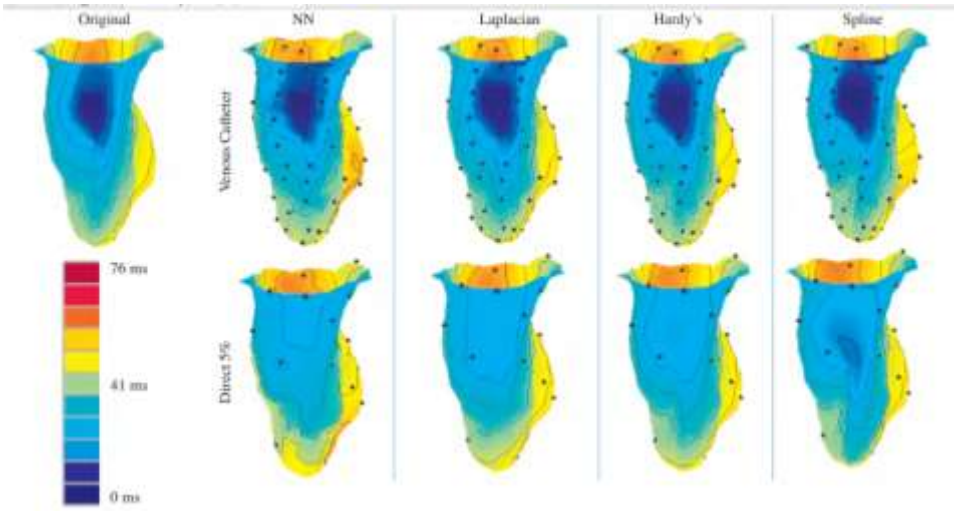

Figure 2. The original activation-time map and the interpolation results of nearest neighbor, Laplacian, Hardy's, and spline approaches on the left endocardium (LE) when the simulation was initialized from a site on the same surface. The surrogate measurements were taken from the 64 basket catheter (MBC) sites and the sites that were regularly distributed over the LE and constituted only 5% of all sites (corresponding to the usage of steerable single catheter).

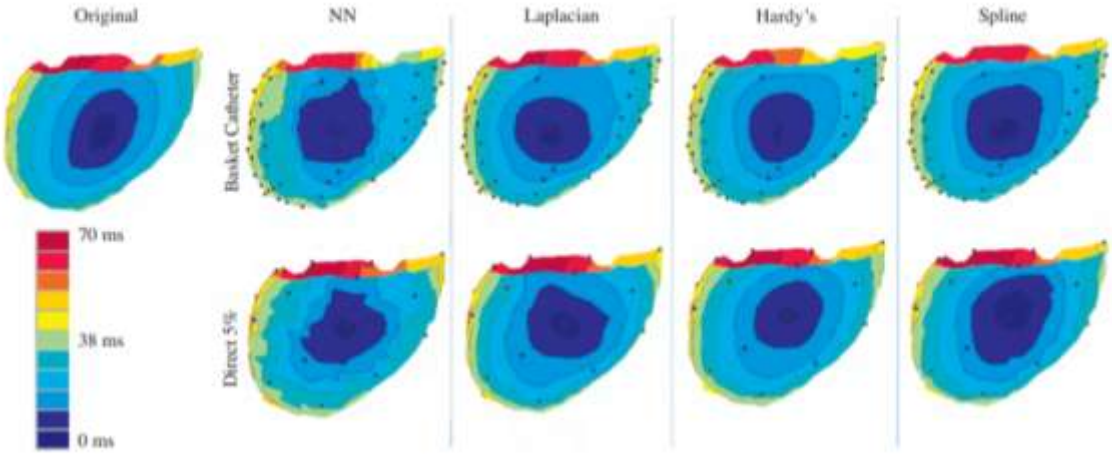

Figure 3. The original activation-time map and the interpolation results of nearest neighbor, Laplacian, Hardy's, and spline approaches on the right endocardium (RE) when the simulation was initialized from a site on the same surface. The surrogate measurements were taken from the 64 basket catheter (MBC) sites and the sites that were regularly distributed over the RE and constituted only the 5% of all sites (corresponding to the usage of steerable single catheter).

Table 1. The results of the statistical comparison of original and interpolated activation-time values for different catheter-types and spatial resolutions for the nearest-neighbor, Laplacian, Hardy's, and spline interpolation methods. The statistical error metrics used were the correlation coefficient (CC), root-mean squared error (RMSE), relative error (RE), and localization error (LocErr). In each cell, the upper value shows the mean value, and the value in the parenthesis shows the standard deviation of the associated metric. The comparisons were performed on the simulated beats originating from the left and right endocardial surfaces (LE and RE), and epicardial surface (Epi).

LE	Nearest Neighboor				Laplacian				Hardy's				Spline			
	CC	RMSE (ms)	RE	LocErr (mm)	CC	RMSE (ms)	RE	LocErr (mm)	CC	RMSE (ms)	RE	LocErr (mm)	CC	RMSE (ms)	RE	LocErr (mm)
5%	0.960 (0.010)	4.389 (0.631)	0.104 (0.016)	5.817 (3.221)	0.986 (0.005)	2.572 (0.474)	0.061 (0.012)	4.125 (2.822)	0.983 (0.008)	2.890 (0.676)	0.068 (0.016)	5.205 (2.971)	0.983 (0.009)	2.798 (0.760)	0.066 (0.019)	4.621 (3.412)
10%	0.970 (0.009)	3.556 (0.556)	0.086 (0.015)	4.228 (2.572)	0.993 (0.002)	1.681 (0.239)	0.041 (0.006)	2.926 (2.154)	0.991 (0.005)	2.000 (0.502)	0.049 (0.013)	3.939 (2.488)	0.992 (0.004)	1.822 (0.422)	0.044 (0.010)	3.117 (2.663)
20%	0.983 (0.004)	2.539 (0.288)	0.065 (0.008)	3.024 (2.145)	0.995 (0.001)	1.296 (0.183)	0.033 (0.005)	2.199 (1.913)	0.995 (0.002)	1.297 (0.253)	0.033 (0.007)	2.723 (2.049)	0.997 (0.001)	1.105 (0.208)	0.028 (0.005)	1.813 (1.844)
MBC	0.978 (0.005)	3.116 (0.318)	0.076 (0.009)	3.840 (2.343)	0.992 (0.003)	1.793 (0.330)	0.044 (0.008)	2.726 (2.298)	0.990 (0.004)	2.041 (0.391)	0.050 (0.010)	3.417 (2.340)	0.987 (0.008)	2.218 (0.698)	0.054 (0.018)	4.298 (4.819)

Table 1. Continued

RE	Nearest Neighboor				Laplacian				Hardy's				Spline			
	CC	RMSE (ms)	RE	LocErr (mm)	CC	RMSE (ms)	RE	LocErr (mm)	CC	RMSE (ms)	RE	LocErr (mm)	CC	RMSE (ms)	RE	LocErr (mm)
5%	0.971 (0.007)	3.722 (0.404)	0.088 (0.010)	5.317 (2.476)	0.990 (0.003)	2.147 (0.263)	0.051 (0.006)	3.441 (2.216)	0.989 (0.003)	2.324 (0.327)	0.055 (0.007)	4.644 (2.403)	0.992 (0.002)	1.891 (0.284)	0.045 (0.006)	3.235 (2.211)
10%	0.974 (0.006)	3.509 (0.530)	0.085 (0.013)	4.234 (2.508)	0.993 (0.002)	1.815 (0.277)	0.044 (0.006)	2.883 (2.243)	0.994 (0.002)	1.745 (0.304)	0.042 (0.007)	3.753 (2.234)	0.996 (0.002)	1.383 (0.266)	0.033 (0.006)	2.574 (2.009)
20%	0.987 (0.003)	2.263 (0.208)	0.058 (0.006)	2.868 (1.887)	0.997 (0.001)	1.123 (0.205)	0.029 (0.005)	1.959 (1.781)	0.997 (0.001)	1.094 (0.222)	0.028 (0.005)	2.656 (1.842)	0.998 (0.001)	0.930 (0.200)	0.024 (0.004)	1.787 (1.783)
MBC	0.955 (0.010)	4.819 (0.876)	0.118 (0.019)	4.359 (3.172)	0.991 (0.004)	1.974 (0.453)	0.049 (0.011)	2.595 (2.138)	0.986 (0.009)	2.687 (1.109)	0.066 (0.025)	3.941 (3.001)	0.993 (0.005)	1.873 (0.686)	0.046 (0.015)	2.760 (2.521)

Epi	Nearest Neighboor				Laplacian				Hardy's				Spline			
	CC	RMSE (ms)	RE	LocErr (mm)	CC	RMSE (ms)	RE	LocErr (mm)	CC	RMSE (ms)	RE	LocErr (mm)	CC	RMSE (ms)	RE	LocErr (mm)
5%	0.995 (0.001)	1.889 (0.132)	0.033 (0.004)	5.202 (2.432)	0.998 (0.000)	1.041 (0.104)	0.018 (0.002)	3.282 (2.037)	0.999 (0.000)	0.911 (0.153)	0.016 (0.003)	4.637 (2.358)	0.999 (0.000)	0.804 (0.117)	0.014 (0.002)	2.586 (1.812)
10%	0.994 (0.001)	2.153 (0.170)	0.039 (0.004)	4.352 (2.559)	0.999 (0.000)	0.903 (0.108)	0.016 (0.002)	2.797 (2.016)	0.999 (0.000)	0.781 (0.164)	0.014 (0.003)	3.767 (2.285)	0.999 (0.000)	0.637 (0.116)	0.011 (0.002)	1.992 (1.728)
20%	0.998 (0.001)	1.221 (0.093)	0.023 (0.003)	2.794 (1.809)	0.999 (0.000)	0.573 (0.058)	0.011 (0.001)	1.954 (1.696)	1.000 (0.000)	0.435 (0.080)	0.008 (0.002)	2.516 (1.748)	1.000 (0.000)	0.368 (0.066)	0.007 (0.001)	1.271 (1.518)
MIVC	0.835 (0.068)	11.068 (2.469)	0.194 (0.039)	14.814 (10.323)	0.950 (0.027)	6.875 (1.720)	0.121 (0.030)	9.561 (5.671)	0.951 (0.046)	6.633 (3.578)	0.114 (0.055)	14.048 (9.700)	0.981 (0.013)	4.030 (0.955)	0.071 (0.019)	5.711 (3.459)

activation-time values, respectively (the associated color bar is included in each figure). Each contour represents an increment of 6 or 8 ms in the activation-time value. The upper rows depict the interpolation results using

multielectrode venous or basket catheter electrodes, and the lower rows show the results of the roving catheter measurements with 5% spatial resolution. The interpolated maps demonstrate similar results with the average values depicted in the table. We note that the contours of interpolated activation maps were smooth and the topographies were similar to the original maps. This was not the case for the nearest-neighbor interpolation scheme. When the MIVC was used to interpolate the epicardial activation-time values and the earliest activation site was away from the surrogate measurement electrodes, the early activated region was shifted towards the catheter electrode locations. Especially with the MIVC, because the right ventricular surface on the epicardium did not have any measurement electrodes, the interpolation schemes such as Laplacian and nearest-neighbor could not reproduce the activation-time values on that surface. On the other hand, the MBC provided an almost regularly distributed sampling; therefore, the interpolation approaches gave relatively successful results. One final note is that spline interpolation performed as good as or in certain cases better than Laplacian and Hardy's interpolation methods, which have been the method of choice in the potential reconstruction on the head, thorax or cardiac surfaces.

DISCUSSION

In this study we investigated the performances of surface interpolation methods, such as the nearest-neighbor, Laplacian, Hardy's, and spline, in the reconstruction of the activation-time values on the epicardial and endocardial inaccessible sites when electrophysiological roving or multielectrode catheters were used for arrhythmia source localization. We evaluated the performances of interpolation methods in terms of resemblance of the original and the reconstructed patterns of activation-time maps and similarity between the original and interpolated activation-time values at the inaccessible sites. Catheter-based activation mapping is extensively used in the electrophysiology laboratories. An acceptable accuracy in interpolation of any point between sparse measurements acquired from catheter electrodes is highly necessary in studying the mechanisms and guiding the therapies of arrhythmias. This study sought to address this issue on the simulated ventricular tachycardia in which ectopic pacing from various epicardial or endocardial sites was performed. In a recent study, Cunedioglu and Yilmaz [23] reported the results from the comparison of simulated activation-time maps extracted from the epicardial surface of the same heart model with the experimental maps obtained from 13 different dogs using a sock electrode array placed on the epicardium. In the experiments the hearts were stimulated from a single site on the epicardium. This comparison showed the similarity in terms of activation-propagation patterns for 470 different focal paced beats in which the average correlation coefficient (CC) was 0.88 (max: 0.97, min: 0.48). This previous study also demonstrated the feasibility of the usage of simulated maps in the investigation of the performance of spatial interpolation methods.

CONCLUSION

1. It is known that 85–95% of the ventricular arrhythmias originate from the endocardial surface [29]. Mapping of endocardial surface utilizing single steerable catheter might be a relatively long procedure. Usingmultielectrode basket or venous catheters on the endocardial surface instead of single steerable catheters might reduce the procedure durations, and thus diminish the exposure to ionizing radiation for both the patient andmedical personnel. However, the employment of the multielectrode catheters brings along the problem of sparse measurement. In this study we propose that in order to reduce the procedure times we might use these catheterstogether with good performance surface interpolation approaches. This approach is advantageous in terms of procedure time, because once the catheters are placed in the chambers or veins and the registration of

the catheter measurement sites with the patient's heart is established, one beat is enough to generate activationtime maps on the associated surface. Using two oblique views of angiography system in the EP laboratory, we would be able to obtain the locations of MBC and MIVC electrodes.In this report we present the usage of spline interpolation method for catheter-based cardiac mapping for the first time. Previously, this approach was shown to be successful in electroencephalography studies. In this problem, spline interpolation performed as well as the Hardy's and Laplacian interpolation approaches.The limitations of this study include that there were no atrial beats or beats from ischemic or infracted hearts in the test set. The hearts were normal and only ectopic pacing was used. In addition, the simulation model did not include the existence of Purkinje fibers, which might complicate the activation maps. However,Ni et al [11] showed that the complexity of the activation maps did not affect the interpolation performances significantly when the performances on the atrial beats and ectopic beats were compared. Moreover, spatial interpolation techniques are limited to reconstruction of maps from the chamber in which the mapping isperformed. As an extension to this study, a volume interpolation approach would be investigated to map the midmyocardial tissue which is located between the epicardial and endocardial surfaces, because a certainpercentage of the arrhythmias are known to originate from the midmyocardium.

REFERENCE

1. M.D. Lesh, G.F. Van Hare, L.M. Epstein, A.P. Fitzpatrick, M.N. Scheinman, R.J. Lee, M.A. Kwasman, H.R. Grogin,MJ.C. Griffin, "Radiofrequency catheter ablation of atrial arrhythmias. Results and mechanisms". Circulation, Vol.89(3), pp. 1074-1089, 1994.
2. D. Darbar, J.E. Olgin, J.M. Miller, P. Friedman, "Localization of the origin of arrhythmias for ablation: From electrocardiography to advanced endocardial mapping systems", J. Cardiovasc. Electrophysiol., Vol. 12(4), pp. 1309–1325, 2001.
3. L. Gepstein, G. Hayam, S.A. Ben-Haim, "A novel method for nonfluoroscopic catheter-based electroanatomical mapping of the heart. In vitro and in vivo accuracy results", Circulation, Vol. 95(1), pp. 1611-1622, 1997.
4. N.M.S. de Groot, M. Bootsma, E.T. van der Velde, M.J. Schalij, "Three-dimensional catheter positioning during radiofrequency ablation in patients: First application of a real-time position management system", J. Cardiovasc.Electrophysiol., Vol. 11, pp. 1183–1192, 2000.
5. M. Eldar, D.G. Ohad, J.J. Goldberger, Z. Rotstein, S. Hsu, D.K. Swanson, A.J. Greenspon, "Transcutaneous multielectrode basket catheter for endocardial mapping and ablation of ventricular tachycardia in the pig", CirculationVol. 96, pp. 2340–2437, 1997.1000
6. G. Arisi, E. Macchi, S. Baruffi, S. Spaggiari, B. Taccardi, "Potential fields on the ventricular surface of the exposed dog heart during normal excitation", Circulation Research, Vol. 52, pp. 706-715, 1983.
7. S.M. Blanchard, R.J. Damiano Jr, W.M. Smith, R.E. Ideker, J.E. Lowe, "Interpolating unipolar epicardial potentials from electrodes separated by increasing distances", PACE, Vol. 12, pp. 1938-1955, 1989
8. R.L. Hardy, "Theory and applications of the multiquadric-biharmonic method", Computers Math. Applic., Vol. 19(8/9), pp. 163-208, 1990.

9. A. van Oosterom, T.F. Oostendorp, G.J. Huiskamp, “Interpolation on a triangulated 3D surface”, J Comp Phys., Vol. 80, pp. 331–343, 1989.
10. R.O. Kuenzler, Generating Epicardial Activation Order from Multielectrode Venous Catheters. M.S. Thesis, Univ. Utah, Salt Lake City, 1998.
11. Alimova, M. F., Qalandarova, D. U., & Alimjonova, L. (2020). CONTEMPORARY ISSUES OF RELIGIOUS STUDIES IN UZBEKISTAN. Solid State Technology, 63(6), 265-272. Alimova, M., & Rakhmonov, S. (2017). ANIMATION–THE IMPORTANT ELEMENT OF PERSPECTIVE DEVELOPMENT OF RURAL TOURISM IN REGIONS OF UZBEKISTAN. THEORETICAL AND PRACTICAL ISSUES OF ENSURING THE ECONOMIC INTERESTS OF THE MODERN INNOVATIVE SOCIETY, 13.
12. KHUDAYBERGANOVA, G. (2018). ASCETICISM IN WORLD RELIGIOUS TRADITIONS. The Light of Islam, 2018(4), 23-28.